

Thermal Creation of Skyrmions in Ferromagnetic Films with Perpendicular Anisotropy and Dzyaloshinskii-Moriya Interaction

Dmitry A. Garanin¹, Eugene M. Chudnovsky¹, Senfu Zhang², and Xixiang Zhang²

¹*Physics Department, Herbert H. Lehman College and Graduate School,
The City University of New York, 250 Bedford Park Boulevard West, Bronx, New York 10468-1589, USA*

²*Physical Science and Engineering Division (PSE),
King Abdullah University of Science and Technology (KAUST), Thuwal 23955-6900, Saudi Arabia*

(Dated: June 17, 2019)

We study theoretically, via Monte Carlo simulations on lattices containing up to 1000×1000 spins, thermal creation of skyrmion lattices in a 2D ferromagnetic film with perpendicular magnetic anisotropy and Dzyaloshinskii-Moriya interaction. At zero temperature, skyrmions only appear in the magnetization process in the presence of static disorder. Thermal fluctuations violate conservation of the topological charge and reduce the effective magnetic anisotropy that tends to suppress skyrmions. In accordance with recent experiments, we find that elevated temperatures assist the formation of skyrmion structures. Once such a structure is formed, it can be frozen into a regular skyrmion lattice by reducing the temperature. We investigate topological properties of skyrmion structures and find the average skyrmion size. Energies of domain and skyrmion states are computed. It is shown that skyrmion lattices have lower energy than labyrinth domains within a narrow field range.

I. INTRODUCTION

Skyrmions are considered for applications in spintronic devices and information processing due to their topological stability¹⁻⁷. Initially introduced in nuclear physics^{8,9}, skyrmions entered magnetism after it was realized¹⁰ that the simplest exchange model in two dimensions (2D) describes topological defects in ferro- and antiferromagnets^{11,12}. During the last decade, magnetic skyrmions have been widely observed in slabs¹³⁻²⁴ and multilayered films²⁵⁻³².

A pure continuous-field 2D exchange model is scale invariant, making the energy of the skyrmion independent of its size. In a solid, the scale invariance is inevitably violated by the crystal lattice and various interactions other than the exchange. Consequently, the energy of the skyrmion becomes dependent on its size. The crystal lattice alone makes the energy of the skyrmion go down with decreasing size, leading to skyrmion collapse³³. Perpendicular magnetic anisotropy, dipole-dipole interaction, magnetic field, and confined geometry can stabilize significantly large magnetic bubbles with skyrmion topology³⁴⁻⁴⁰. The stability of small skyrmions requires other than Heisenberg exchange coupling⁴¹⁻⁴⁵, more complex magnetic anisotropy⁴⁶⁻⁴⁸, static disorder^{49,50}, or a non-centrosymmetric system with large Dzyaloshinskii-Moriya interaction^{5,51-55}.

When working with skyrmions, one of the most challenging tasks is creation of skyrmions in a predictable manner. Creating, annihilating and moving skyrmions by current-induced spin-orbit torques has been the most commonly used method so far, see, e.g., Refs. 7,30,56,57. Skyrmion bubbles have been generated by pushing elongated magnetic domains through a constriction using an in-plane current^{6,58}. Small skyrmions can be also written and deleted in a controlled fashion with local spin-polarized currents from a scanning tunneling

microscope⁵⁹. With a tip of a scanning magnetic force microscope (MFM), one can cut stripe magnetic domains into skyrmions⁶⁰. It has been suggested that individual skyrmions can also be written with an MFM tip⁶¹.

Most recently, thermal methods have been explored. It was shown that light-induced heat pulses of different duration and energy can write skyrmions in a magnetic film in a broad range of temperatures and magnetic fields⁶². In the last years, skyrmions have been observed at relatively high temperatures. This poses a question whether temperature alone can assist the creation of skyrmions. Recently, it has been reported⁶³ that elevated temperature, indeed, facilitates nucleation of skyrmions from the ferromagnetic state and also assists the breaking of magnetic domains into skyrmions in a Pt/Co/Ta film. In this paper we study this problem theoretically by Monte-Carlo calculations on large spin lattices. Our model contains ferromagnetic exchange, Dzyaloshinskii-Moriya interaction (DMI) and perpendicular magnetic anisotropy (PMA). Some of the calculations also include random magnetic anisotropy (RMA) to account for disorder in a real film.

The first comprehensive study of two-dimensional vortex lattices in systems with DMI and uniaxial magnetic anisotropy was done by Bogdanov and Hubert⁶⁴ within continuous micromagnetic theory. By considering cylindrically symmetric solutions for individual vortices, they found the dependence of their profile on the strength of the DMI, anisotropy, and the external field. Energies of the periodic arrangement of vortices have been computed and compared with energies of other states to obtain the magnetic phase diagram. More recently the effects of thermal fluctuations and topological charge associated with vortex lattices have been addressed. Yu et al.¹⁷ used Monte Carlo simulations to explain images of skyrmion phases that they obtained experimentally with the help of the real-space Lorentz TEM of FeCoSi films.

By varying temperature and magnetic field they observed transitions between uniformly magnetized states, laminar domains, and skyrmion crystals. A skyrmion tube crystal as a thermodynamically equilibrium phase of a 3D $30 \times 30 \times 30$ anisotropic chiral spin lattice has been found by Monte Carlo method by Buhrandt and Fritz⁶⁵. An important observation made in this paper (that we confirm by Monte Carlo simulations of much larger 2D spin lattices) is that thermal fluctuations alone can generate a skyrmion state in a narrow region of the field-temperature phase diagram. Stability of individual skyrmions against thermal fluctuations has been studied within the discrete Heisenberg model by Hagemeister et al.⁶⁶. By employing stochastic Landau-Lifshitz equation, Rózsa et al.⁶⁷ investigated skyrmion lifetime. They also employed Monte Carlo simulations to study creation and annihilation of skyrmions on 128×128 lattices and computed multi-skyrmion spin configurations, including topological charge. Most recently Böttcher et al.⁶⁸ reported parallel-tempering Monte Carlo studies of the temperature dependence of magnetization and topological charge, as well as the field-temperature phase diagram of Pd/Fe/Ir films. They observed formation of both skyrmions and antiskyrmions at high temperatures.

Our goal is to analyze how thermally assisted skyrmion states depend on temperature, the external magnetic field, and the PMA in a basic Heisenberg model with DMI when the field is cycled along the hysteresis loop, without trying to compute the equilibrium phase diagram (that is more of a theoretical abstraction in a magnetic system with hysteresis). It is achieved by computing the total topological charge along the magnetization curve on large (up to 1000×1000) 2D spin lattices and by illustrating skyrmion states with images of the spin field and images of the topological charge density. We clarify the role of the PMA and compare efficiencies of the static disorder and temperature in creating skyrmions in the magnetization process. We show that fluctuating spin-field obtained at elevated temperatures can be frozen into a regular skyrmion lattice by reducing the temperature. Concentration of skyrmions and their size depend on the external field and on the PMA. Since the system exhibits profound magnetic hysteresis, with many local energy minima corresponding to various spin configurations, it makes sense to compare energies of skyrmion states with energies of the domain states. In accordance with experiment⁶³ and with previously reported theoretical results, we find that skyrmion states win in a narrow field range.

This paper is organized as follows. The model and numerical method are discussed in Section II. Spin states emerging along the magnetization curve at zero temperature are studied in Section III, where also the field dependence of the topological charge is computed with and without static disorder in the film. Finite-temperature effects are studied in Section IV. In that Section, we compute the dependence of the hysteresis curves and topological charge on temperature and PMA, and inves-

tigate topology of frozen skyrmion states. Properties of skyrmion lattices and their energies vs energies of domain states are computed and compared in Section V. Our conclusions and suggestions for experiment are discussed in Section VI.

II. THE MODEL AND NUMERICAL METHOD

We study the lattice spin model with a Hamiltonian

$$\begin{aligned} \mathcal{H} = & -\frac{J}{2} \sum_{ij} \mathbf{s}_i \cdot \mathbf{s}_j - H \sum_i s_{iz} - \frac{D}{2} \sum_i s_{iz}^2 \\ & + A \sum_i [(\mathbf{s}_i \times \mathbf{s}_{i+\hat{x}}) \cdot \hat{x} + (\mathbf{s}_i \times \mathbf{s}_{i+\hat{y}}) \cdot \hat{y}] \\ & - \frac{D_R}{2} \sum_i (\mathbf{n}_{Ri} \cdot \mathbf{s}_i)^2 - \frac{E_D}{2} \sum_{ij} \phi_{ij,\alpha\beta} s_{i\alpha} s_{j\beta}. \end{aligned} \quad (1)$$

Here the first term represents the exchange interaction between the nearest neighbors, with \mathbf{s}_i being the spin at the i -th site of the crystal lattice and J being the exchange constant. The second term is the Zeeman interaction of the spins with magnetic field applied in the z -direction, perpendicular to the xy -plane of the film. Here $H \equiv g\mu_B SB$, S is the value of the atomic spin, B is the induction of the applied magnetic field, and g is the gyromagnetic factor. The third term accounts for the PMA of strength D . (In our computations the atomic-scale RMA is used, that is, the direction of the RMA axis is assumed random at any lattice site, with its strength being constant. One can also use the model with a correlated RMA that has a stronger effect. The latter allows the use of a smaller anisotropy constant to achieve a similar effect.) The fourth term describes the Bloch-type DMI⁵ of strength A . For the Néel-type DMI it should be replaced with $A \sum_i [(\mathbf{s}_i \times \mathbf{s}_{i+\hat{x}}) \cdot \hat{y} - (\mathbf{s}_i \times \mathbf{s}_{i+\hat{y}}) \cdot \hat{x}]$. The fifth term incorporates the effect of the RMA of strength D_R , with \mathbf{n}_{Ri} describing a randomly chosen orientation of the anisotropy axis at the i -th lattice site. The last term is the DDI with

$$\phi_{ij,\alpha\beta} \equiv a^3 r_{ij}^{-5} (3r_{ij,\alpha} r_{ij,\beta} - \delta_{\alpha\beta} r_{ij}^2). \quad (2)$$

Here r_{ij} is the distance between the i -th and the j -th site, a is the lattice spacing, $\alpha, \beta = x, y, z$ denotes spin components, and $E_D = \mu_0 M_0^2 a^3 / (4\pi)$ is the strength of the DDI (with μ_0 being the magnetic permeability of vacuum and M_0 being the saturation magnetization, $M_0 = g\mu_B S/a^3$ for our lattice model). In all our computations, we have found that the effect of the DMI on spin configurations dominates over the competing effect of a much weaker DDI.

To describe non-uniform spin states, one needs to consider a system with a large number of spins. In the lattice model, this leads to long computation times. For many materials the problem is further exacerbated by the weakness such interactions as DMI, Zeeman, PMA, RMA, and DDI in comparison with the ferromagnetic

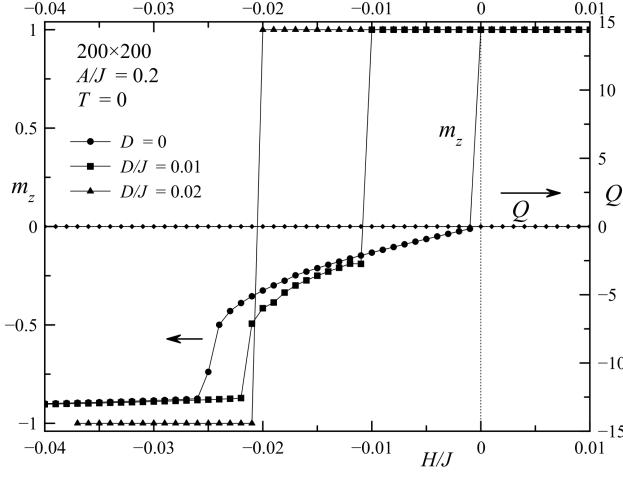


Figure 1: Magnetization curves and topological charge at $T = 0$ in the model with DMI and PMA.

exchange. It makes the system magnetically soft, further slowing down the convergence towards the energy minimum in the computation routine. In such materials the emerging spin structures are large compared to the atomic spacing a . When interactions are small, to speed up computation, one can rescale the 2D problem to the same problem with a bigger lattice constant $b > a$ and new parameters $J' = J$, $A' = (b/a)A$, $H' = (b/a)^2 H$, $D' = (b/a)^2 D$. The rescaled problem has a smaller number of mesh points $N'_\alpha = (a/b)N_\alpha$ and smaller mismatch between J and other interaction constants. The results of the computation can be easily rescaled back to the original model.

In what follows we use $A/J = 0.2$, $D/J = 0$ or 0.01 or 0.02 , and $D_R/J = 0$ or 0.3 , and set $J = 1$, $s = 1$. Calculations have been performed on 2D lattices of size up to 300×300 .

Among other features we are interested in the topological charge of the emerging spin structures. In a continuous spin-field model it is given by¹⁰

$$Q = \int dx dy q(x, y), \quad q(x, y) = \frac{1}{4\pi} \mathbf{s} \cdot \frac{\partial \mathbf{s}}{\partial x} \times \frac{\partial \mathbf{s}}{\partial y}. \quad (3)$$

The number Q takes discrete values $Q = 0, \pm 1, \pm 2, \dots$. The function $q(x, y)$ can be interpreted as the density of the topological charge. It provides a better visualization of the location of skyrmions and antiskyrmions when they are strongly deformed from the minimum-energy Belavin-Polyakov (BP) shape by disorder and competing interactions and cannot be easily identified by looking at the spin field⁴⁹. In numerical work we use a lattice-discretized version of Eq. (3).

At zero temperature, we compute minimum-energy configurations of spins. Our numerical method combines sequential rotations of spins \mathbf{s}_i towards the direction of the local effective field, $\mathbf{H}_{\text{eff},i} = -\partial \mathcal{H} / \partial \mathbf{s}_i$, with the probability α , and the energy-conserving spin flips (so-called

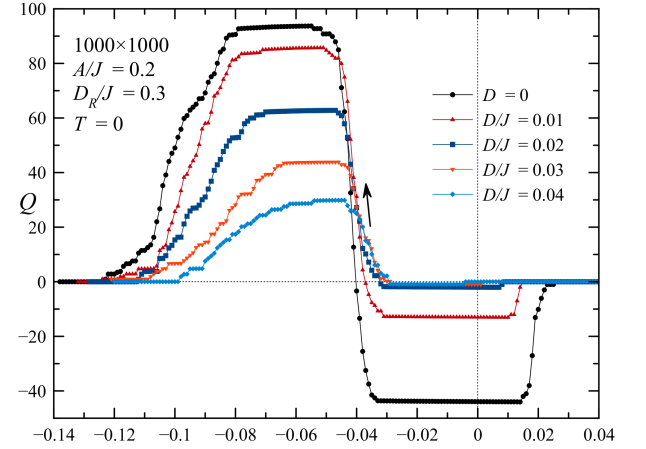
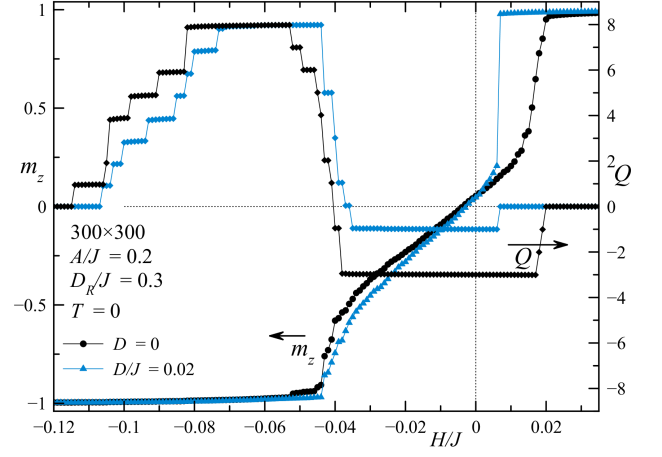


Figure 2: Magnetization curves and topological charge at $T = 0$ in the model with DMI, PMA, and RMA. Upper panel: 300×300 lattice. Lower panel: Topological charge in a 1000×1000 lattice with many more skyrmions.

overrelaxation), $\mathbf{s}_i \rightarrow 2(\mathbf{s}_i \cdot \mathbf{H}_{\text{eff},i})\mathbf{H}_{\text{eff},i}/H_{\text{eff},i}^2 - \mathbf{s}_i$, with the probability $1 - \alpha$. The parameter α plays the role of the effective relaxation constant. We mainly use the value $\alpha = 0.03$ that provides the overall fastest convergence. At nonzero temperatures, we replace the rotation of spins towards the direction of the effective field by Monte Carlo updates, keeping the over-relaxation dominant via the same small value of α . We change the field in small steps and allow the system to reach (metastable) equilibrium at each step. This is equivalent to a slow field sweep in experiment. Due to the large system size, thermodynamic fluctuations and the statistical scatter are small, making the predicted features reliable with a large degree of confidence.

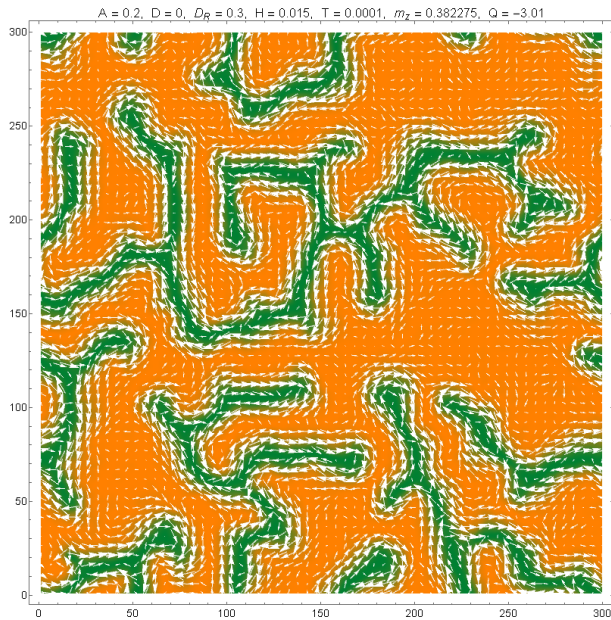


Figure 3: Proliferation of worm-like domains at $T = 0$ in the model with DMI and RMA at $H > 0$. Orange/green color indicates positive/negative z -component of the spin field. The in-plane spin components are shown as white arrows.

III. SPIN STATES AT ZERO TEMPERATURE

Fig. 1 shows the numerical results for the reduced magnetization per spin $m_z = \langle s_z \rangle$ (left axis), with the average taken over all lattice sites, and the total topological charge Q (right axis) at $T = 0$. As H decreases from saturation, the uniform state with $m_z = 1$ becomes unstable and the system jumps into the state with laminar domains created by the DMI. As the field continues to change, this domain structure becomes gradually suppressed, leading to the uniformly magnetized state with $m_z = -1$ at the field saturating the system in the negative z -direction. In the case of zero anisotropy, $D = 0$, the instability of the uniformly magnetized state occurs exactly at $H = 0$. Finite PMA makes the uniform state more stable, so that the instability occurs at $H = -D$ when the applied field compensates the effective anisotropy field. One can see that $Q = 0$ at $T = 0$ everywhere along the magnetization curve. This is a consequence of the conservation of the topological charge in the absence of thermal or static randomness.

The effect of static randomness at $T = 0$, generated by the RMA, is illustrated in Fig. 2. One can see that in the absence of the PMA, the RMA is triggering the instability of the quasi-uniformly magnetized state with $m_z \approx 1$ already at $H > 0$. The destruction of the uniformly magnetized state leads to the proliferation of worm-like domains, see Fig. 3, with a non-zero though small topological charge per unit area. According to Fig. 2 a non-zero PMA with $D/J = 0.02$ increases the stability range of the uniformly magnetized state and reduces Q of the do-

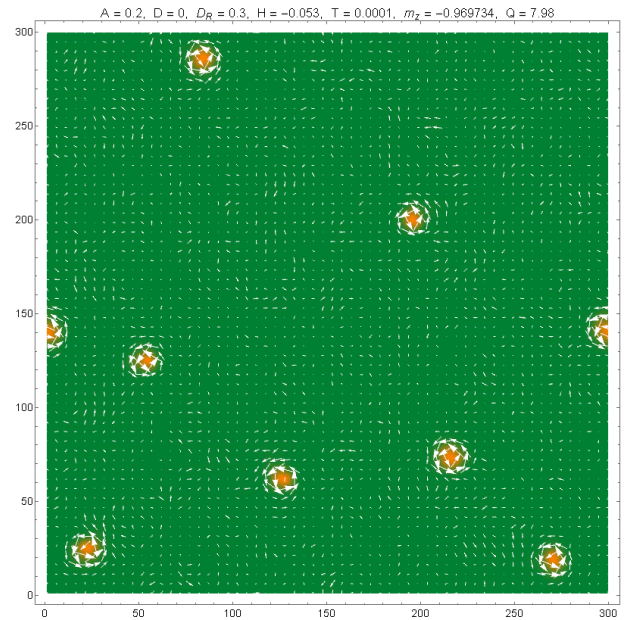


Figure 4: Small number of skyrmions resulting from the breaking of labyrinth domains by the magnetic field, $H < 0$, in the presence of RMA at $T = 0$.

main state even further. The scaling of the effect with the area of the film is illustrated by the lower panel of Fig. 2 that shows a significantly greater Q and a smoother dependence on the field due to many more skyrmions generated in a larger 1000×1000 spin lattice.

As the magnetic field switches towards the negative direction, while changing continuously along the magnetization curve (see Fig. 2), some domains break into skyrmions, creating a few skyrmions shown in Fig. 4. While skyrmions do not appear spontaneously at $T = 0$ in the absence of RMA, the maximum number of skyrmions emerging in the magnetization process from labyrinth domains in the presence of RMA is still small at $T = 0$. As we shall see below, temperature has a much more profound effect on the emergence of skyrmions.

IV. SPIN STATES AT FINITE TEMPERATURE

We will now turn to the creation of skyrmions at finite temperature. The effect of temperature is two-fold. Firstly, thermal fluctuations violate conservation of the topological charge even in the pure exchange model. Secondly, spin fluctuations reduce the effective PMA that tends to suppress skyrmions. As we shall see, they first emerge via thermal nucleation from the uniformly magnetized state and then when the destruction of ferromagnetic domains by the magnetic field is assisted by temperature.

Fig. 5 shows the dependence of $m_z(H)$ and $Q(H)$ in the model with DMI and no PMA at different temperatures. At $T/J = 0.5$ and 0.4 the system is approximately

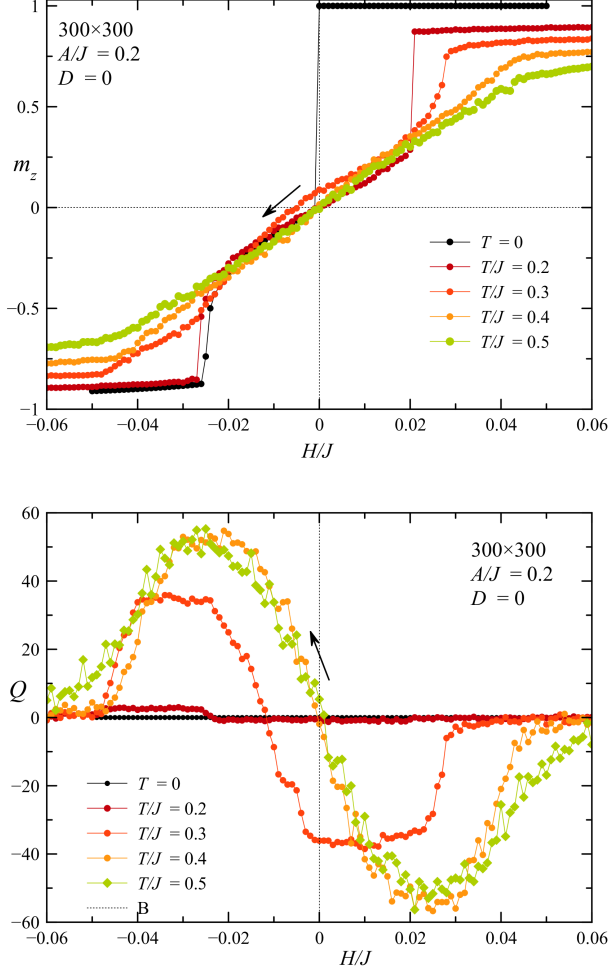


Figure 5: Magnetization curves (upper panel) and topological charge (lower panel) at finite temperature in the model with DMI at $D = 0$.

in thermal equilibrium at any H , so that the magnetization curve is reversible. At lower temperatures, the equilibrium cannot be achieved within a reasonable time of Monte Carlo simulations and the reversibility is lost, which reflects the physics of the magnetic hysteresis. The value of $T/J = 0.3$ is an intermediate one for which a partial thermal equilibrium is achieved. One can see that the number of created skyrmions decreases at low temperatures, so that the results presented in Fig. 1 are recovered.

Finite temperatures cause nucleation of skyrmions at $H > 0$ with a rather large topological charge Q of the entire film, see Fig. 6. As the magnetic moments of these skyrmions point down against the spin-up background, Q is negative. Decreasing the field towards $H \approx 0$ increases skyrmion concentration until skyrmions begin to merge into magnetic domains, see Fig. 7, and the topological charge of the film drops. As the field increases in the negative direction, the domains begin to break back into

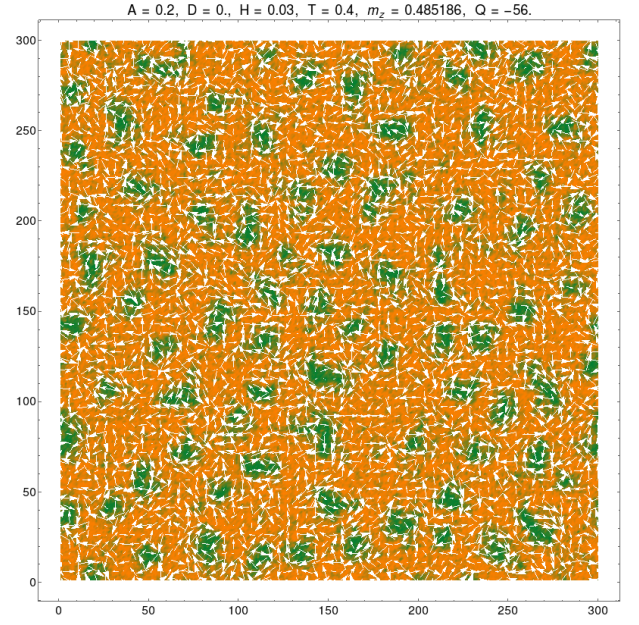


Figure 6: Thermally nucleated skyrmions at $T/J = 0.4$, $D = 0$, and $H/J = 0.03$.

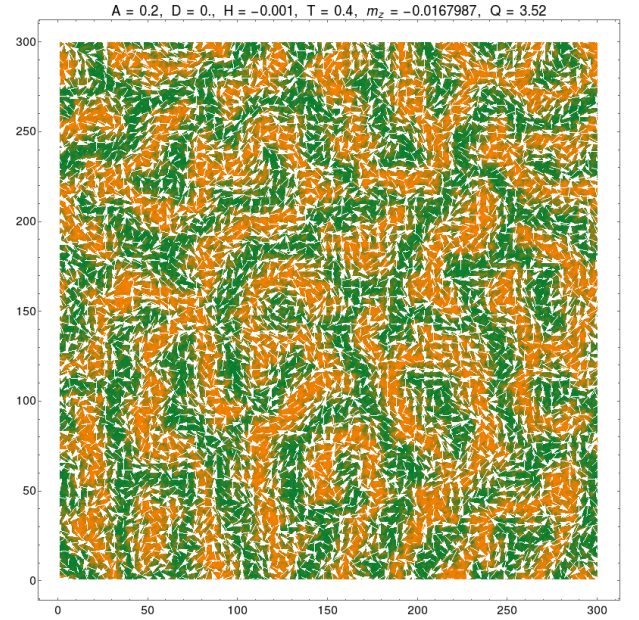


Figure 7: Labyrinth domains from merging skyrmions at $T/J = 0.4$, $D = 0$, and $H/J = -0.001$.

skyrmions, making Q positive and large again, see Fig. 8. Skyrmions collapse as the magnetization of the film approaches saturation. Note that at elevated temperatures spin configurations fluctuate. The pictures above show snapshots of such configurations.

Fig. 9 shows the results of similar computations with a finite PMA of strength $D/J = 0.02$. The latter strongly suppresses skyrmions, their number becoming significant only at elevated temperatures such as $T/J = 0.5$, when

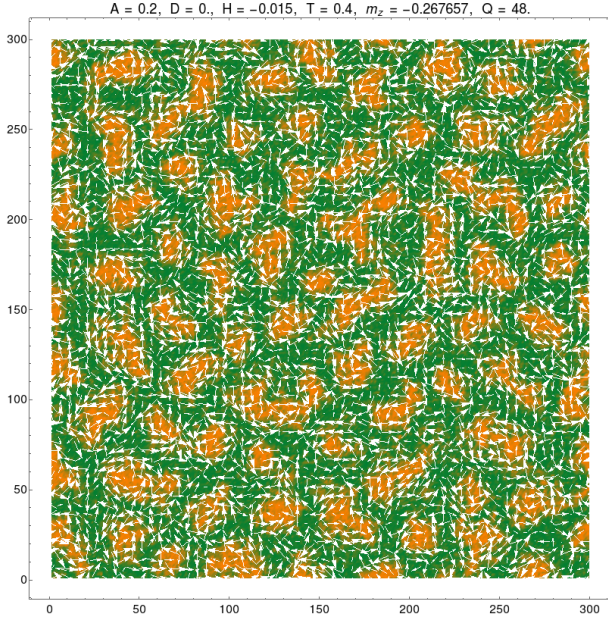


Figure 8: Thermally assisted formation of skyrmions from labyrinth domains broken by the field at $T/J = 0.4$, $D = 0$, and $H/J = -0.015$.

thermodynamic equilibrium in Monte Carlo simulations is still incomplete.

We also have performed numerical experiments that simulate freezing of the fluctuating skyrmion states obtained at elevated temperatures down to $T = 0$, which is similar to the protocol of some real experiments with skyrmions^{22,69}. An example of the freezing of the skyrmion state generated at $H/J = -0.015$ and $T/J = 0.4$ (see Fig. 8) is shown in Fig. 10. In this example, the freezing leads to an imperfect skyrmion lattice. Similar numerical experiment at $H/J = -0.025$ and $T = 0$, obtained from the random-spin state at $T = \infty$ as the initial condition for the relaxation, leads to a more regular skyrmion lattice with a larger number of smaller skyrmions, see Fig. 11.

V. SKYRMION LATTICES VS LABYRINTH DOMAINS

In a different numerical experiment, we investigated skyrmion states at $T = 0$ evolving on changing the applied field H in both directions in small steps starting from the state shown in Fig. 11. Initially, 90-100 skyrmions emerged in the 300×300 lattice at $H/J = -0.025$. Decreasing the field from the initial value, makes skyrmions smaller and eventually leads to their collapse. Increasing the field makes skyrmions larger. When they come in contact with each other, the regular skyrmion lattice transforms into densely packed skyrmions of various size shown in Fig. 12. On further increase of the field the walls separating skyrmion bubbles become thinner.

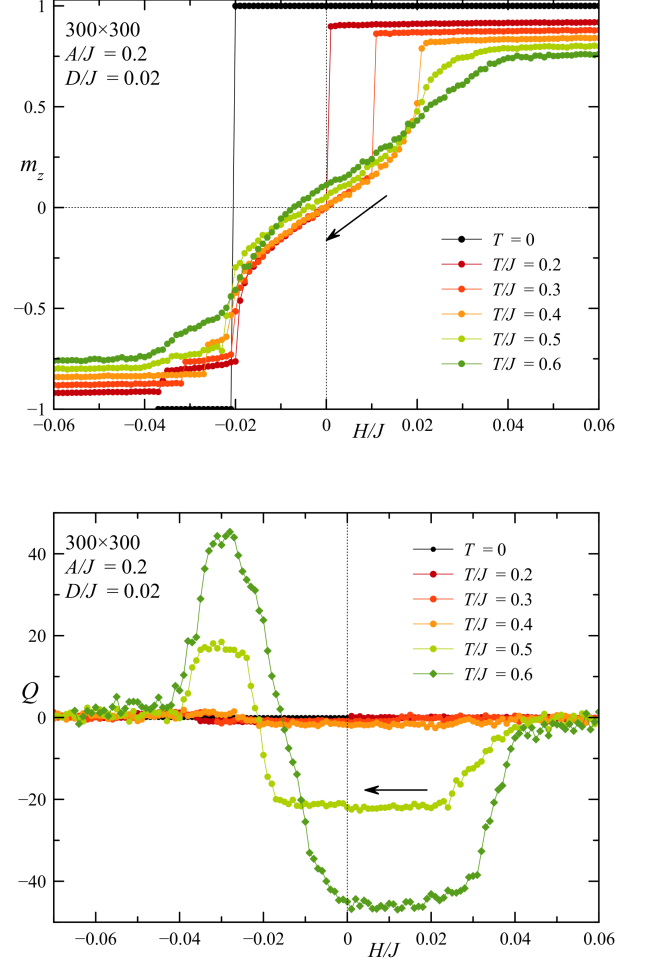


Figure 9: Magnetization curves (upper panel) and topological charge (lower panel) at finite temperature in the model with DMI and PMA.

As the field continues to grow, skyrmion walls collapse in a single large jump leading to a quasi-uniform magnetization.

In a systems with a strong DMI, the number of skyrmions at $T = 0$ equals Q and can be counted easily. The effective radius of the skyrmion bubble that does not have a BP shape can be estimated using the formula for a thin-wall bubble,

$$\pi Q R_{\text{eff}}^2 = \frac{1}{2} \int \int dx dy [1 \pm s_z(x, y)], \quad (4)$$

if $s_z = \mp 1$ in the background. To make this formula more robust for elevated temperatures, when s_z in the background deviates from ± 1 due to thermal fluctuations, one can replace $s_z(x, y)$ in Eq. (4) with ± 1 depending on its sign. However, at elevated temperatures, while Q remains a well-defined reproducible quantity, there is a significant washing-out of the TCD, as Eq. (3) contains two derivatives and the spin field changes at the lattice

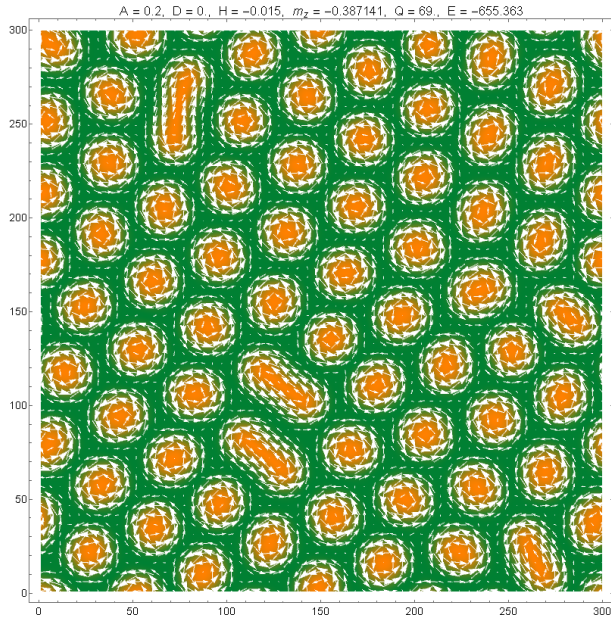


Figure 10: Skyrmion lattice obtained by freezing down to $T = 0$ the thermally assisted skyrmion state shown in Fig. 8.

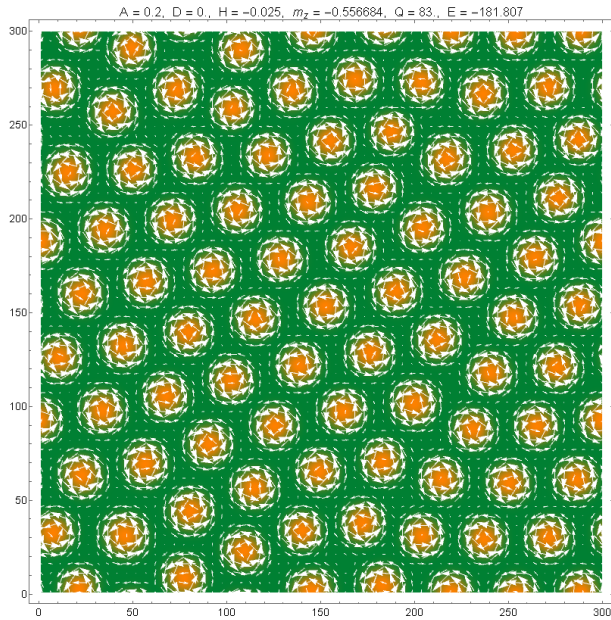


Figure 11: Skyrmion lattice obtained at $H/J = -0.025$ by freezing down to $T = 0$ the random-spin state at $T = \infty$.

scale. This is confirmed by looking at the density of the topological charge plotted in the upper panel of Fig. 13 for the skyrmion lattice shown in the lower panel of that figure. At higher temperatures, the TCD washes out completely due to strong spin fluctuations at the atomic-scale. Still, the integral value of Q turns out to be robust and consistent with the number of skyrmions one can count in the image of spin field similar to the one shown in the lower panel of Fig. 13.

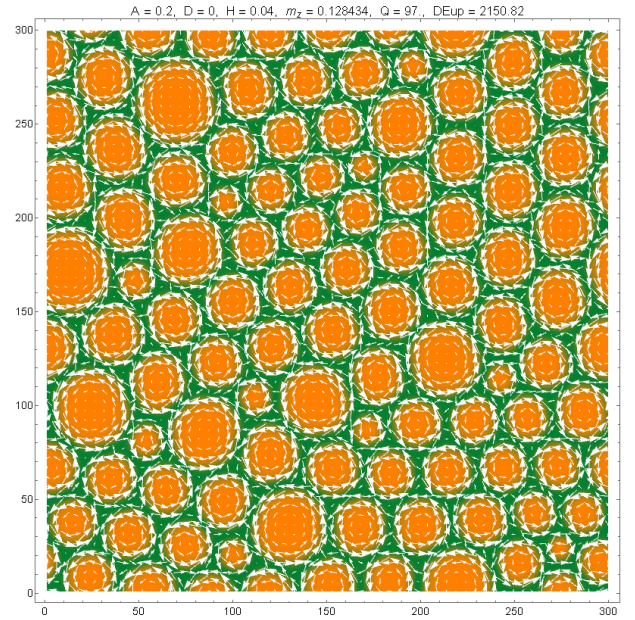


Figure 12: Metastable skyrmion state that evolved on increasing the field from the skyrmion lattice at $H/J = -0.025$ shown in Fig. 11. The skyrmion structure is shown at $H/J = 0.04$ that is close to the critical field at which the walls between the skyrmion bubbles collapse.

The dependence of R_{eff} on H for $D/J = 0.02$ and 0 is shown in Fig. 14. For the model with anisotropy R_{eff} is smaller and the collapse on the left side occurs earlier. This can be understood in simple terms within the continuous spin-field model. If one neglects the dependence of the exchange energy on skyrmion size and neglects interaction between skyrmions, the DMI energy of the skyrmion scales as $-AR_{\text{eff}}$ while the PMA+ Zeeman energy scales as $(D + |H|)R_{\text{eff}}^2$. (This scaling of the PMA assumes $R_{\text{eff}} < \delta$, where $\delta = \sqrt{J/D}$ is the domain wall width.) The energy minimum is achieved at $R_{\text{eff}} \propto A/(D + |H|)$, which agrees qualitatively with Fig. 14 as long as $H < 0$ and is sufficiently strong. At $D = 0$ and $H \rightarrow 0$, the formula for R_{eff} above diverges. Before it happens, skyrmions evolve into labyrinth domains. The skyrmion lattice at $H > 0$ is stable due to the interaction between the skyrmions. On increasing the field the skyrmions grow and become densely packed, see Fig. 12. They burst at the well defined field, leading to the uniform magnetization. This corresponds to the right-hand end of the $R_{\text{eff}}(H)$ curve in Fig. 14.

Next we compare energies of the skyrmion and domain states. In Fig. 15 they are plotted as function of the field with respect to the energy of the uniformly magnetized state with spins directed up or down. The skyrmion lattice has the energy lower than the domain structure and lower than the uniformly magnetized state in a narrow range of negative fields that becomes more narrow with increasing PMA.

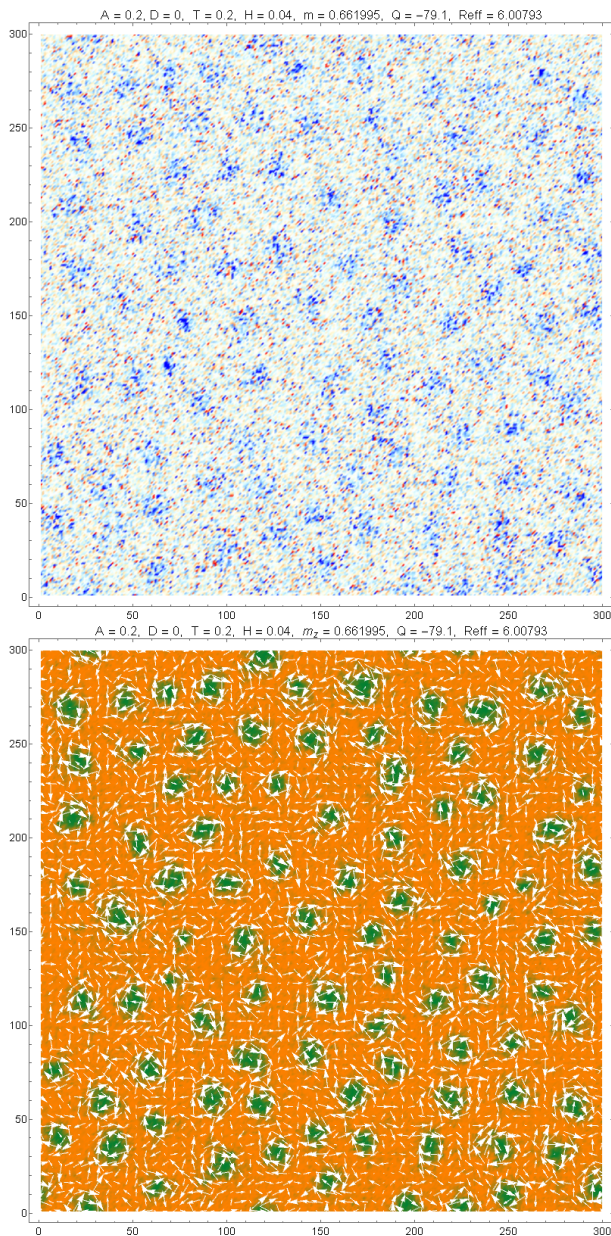


Figure 13: Topological charge density (TCD) (upper panel) for the skyrmion lattice shown in the lower panel. The color code in the TCD plot is red for positive TCD and blue for negative TCD.

VI. DISCUSSION

We have studied theoretically, via Monte Carlo simulations on large spin lattices, the skyrmion states that emerge along the hysteresis curve in a ferromagnetic film with the DMI, PMA, and RMA at zero and finite temperatures. Our results agree with recent experimental findings⁶³ on thermally assisted creation of skyrmions, thus providing theoretical background for these findings.

In accordance with experiments, we find two mechanisms of the creation of skyrmions: 1) via thermally as-

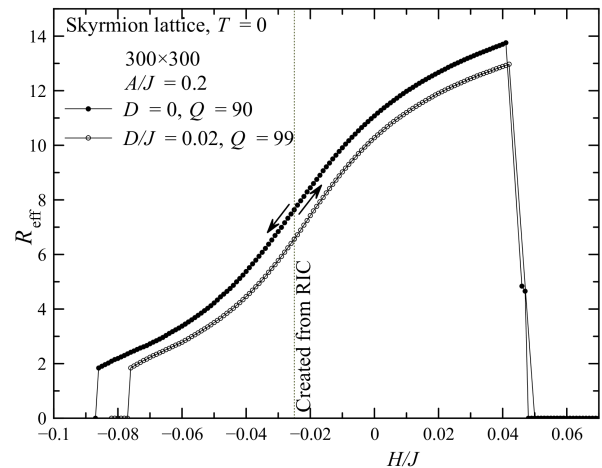


Figure 14: Field dependence of the effective radius of skyrmions in the skyrmion lattice created from the RIC at $T = 0$ with $D/J = 0$ and 0.02 on increasing and decreasing the field from the initial value $H/J = -0.025$.

sisted nucleation from the uniformly magnetized state and 2) via destruction of labyrinth magnetic domains into skyrmions. These skyrmion states appear in positive and negative fields respectively along the magnetization curve. In Ref. 63, the temperature dependence of the PMA has been independently measured and the correlation of the amplitude of the PMA with the field range where skyrmions exist has been found.

In our studies we choose the zero-temperature value of the PMA as a microscopic parameter and obtain the decrease of the effective PMA with temperature self-consistently, owed to thermal fluctuations of the spins. In agreement with experiment, we find that in a system without quenched randomness the skyrmion states exist in a narrow field range suppressed by the PMA.

At $T = 0$ conservation of the topological charge suppresses creation of skyrmions unless static randomness is present in the system. We model such randomness by the RMA. In contrast with the PMA, the RMA, similarly to the temperature but not as effective, creates a non-zero topological charge in a broad field range even at $T = 0$. While our results agree qualitatively with a large body of previous work on skyrmion states, see, e.g., Ref. 5, the account of the temperature dependence of the magnetic anisotropy and of the effect of random magnetic anisotropy provide important new nuances to this problem.

We have observed in numerical experiments how skyrmions merge into labyrinth domains and how the domains decay back into skyrmions on changing the field. Properties of skyrmion states depend strongly on the manner in which they are obtained. We have studied skyrmion lattices generated by changing the field along the hysteresis curve, formation of skyrmion structures assisted by static randomness, by temperature, by freezing

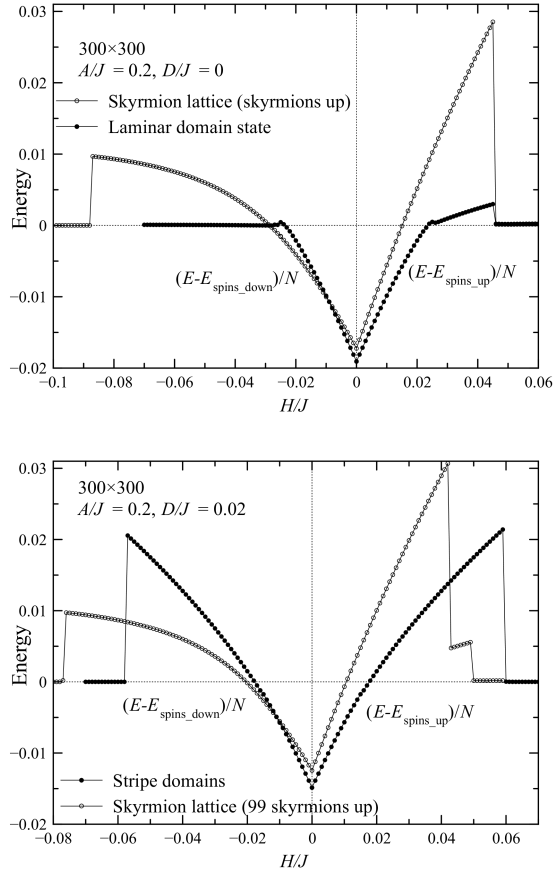


Figure 15: Energy of the skyrmion lattice (skymions pointing up against the spin-down background) and the domain state with respect to the energy of the uniformly magnetized state with the spins up or down. The skyrmion lattice is the ground state in a narrow region of negative fields. Upper panel: $D = 0$. Lower panel: $D/J = 0.02$.

the system from elevated temperature to $T = 0$, as well as skyrmion lattices emerging from random initial conditions for the spins.

The work on skyrmionics, that began at low temperatures, has now moved to room temperatures and above. This has made possible the experiments on thermally assisted creation of skyrmions, like the ones described in Ref. 63. We hope that the findings reported in this paper will further assist planning and understanding of such experiments.

VII. ACKNOWLEDGEMENTS

This work has been supported by the grant No. OSR-2016-CRG5-2977 from King Abdullah University of Science and Technology.

- ¹ N. Nagaosa and Y. Tokura, Topological properties and dynamics of magnetic skyrmions, *Nature Nanotechnology* **8**, 899-911 (2013).
- ² R. Tomasello, E. Martinez, R. Zivieri, L. Torres, M. Carpentieri, and G. Finocchio, A strategy for the design of skyrmion racetrack memories, *Nature Scientific Reports* **4**, 6784-(7) (2014).
- ³ X. Zhang, M. Ezawa, and Y. Zhou, Magnetic skyrmion logic gates: conversion, duplication and merging of skyrmions, *Scientific Reports* **5**, 9400-(8) (2015).
- ⁴ G. Finocchio, F. Büttner, R. Tomasello, M. Carpentieri, and M. Klau, Magnetic skyrmions: from fundamental to applications, *Journal of Physics D: Applied Physics*. **49**, 423001-(17) (2016).
- ⁵ A. O. Leonov, T. L. Monchesky, N. Romming, A. Kubetzka, A. N. Bogdanov, and R. Wiesendanger, The properties of isolated chiral skyrmions in thin magnetic films, *New Journal of Physics* **18**, 065003-(16) (2016).
- ⁶ W. Jiang, G. Chen, K. Liu, J. Zang, S. G. E. te Velthuis,

- and A. Hoffmann, Skyrmions in magnetic multilayers, *Physics Reports* **704**, 1 - 49 (2017).
- ⁷ A. Fert, N. Reyren, and V. Cros, Magnetic skyrmions: advances in physics and potential applications, *Nature Reviews Materials* **2**, 17031-(15) (2017).
- ⁸ T. H. R. Skyrme, A non-linear theory of strong interactions, *Proceedings of the Royal Society A* **247**, 260-278 (1958).
- ⁹ A. M. Polyakov, *Gauge Fields and Strings*, Harwood Academic Publishers 1987.
- ¹⁰ A. A. Belavin and A. M. Polyakov, Metastable states of two-dimensional isotropic ferromagnets, *Pis'ma Zh. Eksp. Teor. Fiz* **22**, 503-506 (1975) [*JETP Lett.* **22**, 245-248 (1975)].
- ¹¹ E. M. Chudnovsky and J. Tejada, *Lectures on Magnetism*, Rinton Press (Princeton - NJ, 2006).
- ¹² Book: *The Multifaceted Skyrmion*, edited by G. E. Brown and M. Rho (World Scientific, 2010).
- ¹³ S. V. Grigoriev, V. Dyadkin, E. Moskvina, D. Lamago, T.

- Wolf, H. Eckerlebe, and S. Maleyev, Helical spin structure of $\text{Mn}_{1-y}\text{Fe}_y\text{Si}$ under a magnetic field: Small angle neutron diffraction study, *Physical Review B* **79**, 144417-(10) (2009).
- ¹⁴ C. Pappas, E. Lelièvre-Berna, P. Falus, P. Bentley, E. Moskvina, S. Grigoriev, P. Fouquet, and B. Farago, Chiral paramagnetic skyrmion-like phase in MnSi, *Physical Review Letters* **102**, 197202-(4) (2009).
 - ¹⁵ F. Jonietz, S. Mühlbauer, C. Pfleiderer, A. Neubauer, W. Münzer, A. Bauer, T. Adams, R. Georgii, P. Böni, and R. Duine, Spin transfer torques in MnSi at ultralow current densities, *Science* **330**, 1648 - 1651 (2010).
 - ¹⁶ W. Münzer, A. Neubauer, T. Adams, S. Mühlbauer, C. Franz, F. Jonietz, R. Georgii, P. Böni, B. Pedersen, and M. Schmidt, Skyrmion lattice in the doped semiconductor $\text{Fe}_{1-x}\text{Co}_x\text{Si}$, *Physical Review B* **81**, R041203-(4) (2010).
 - ¹⁷ X. Yu, Y. Onose, N. Kanazawa, J. Park, J. Han, Y. Matsui, N. Nagaosa, and Y. Tokura, Real-space observation of a two-dimensional skyrmion crystal, *Nature* **465**, 901 - 904 (2010).
 - ¹⁸ N. Kanazawa, Y. Onose, T. Arima, D. Okuyama, K. Ohoyama, S. Wakimoto, K. Kakurai, S. Ishiwata, and Y. Tokura, Large topological Hall effect in a short-period helimagnet MnGe, *Physical Review Letters* **106**, 156603-(4) (2011).
 - ¹⁹ X. Yu, N. Kanazawa, Y. Onose, K. Kimoto, W. Zhang, S. Ishiwata, Y. Matsui, and Y. Tokura, Near room-temperature formation of a skyrmion crystal in thin-films of the helimagnet FeGe, *Nature Materials* **10**, 106 - 109 (2011).
 - ²⁰ A. Tonomura, X. Yu, K. Yanagisawa, T. Matsuda, Y. Onose, N. Kanazawa, H. S. Park, and Y. Tokura, Real-space observation of skyrmion lattice in helimagnet MnSi thin samples, *Nano Letters* **12**, 1673 -1677 (2012).
 - ²¹ X. Yu, N. Kanazawa, W. Zhang, T. Nagai, T. Hara, K. Kimoto, Y. Matsui, Y. Onose, and Y. Tokura, Skyrmion flow near room temperature in an ultralow current density, *Nature Communications* **3**, 988 (2012).
 - ²² P. Milde, D. Köhler, J. Seidel, L. Eng, A. Bauer, A. Chacon, J. Kindervater, S. Mühlbauer, C. Pfleiderer, and S. Buhrandt, Unwinding of a skyrmion lattice by magnetic monopoles, *Science* **340**, 1076 -1080 (2013).
 - ²³ K. Shibata, X. Yu, T. Hara, D. Morikawa, N. Kanazawa, K. Kimoto, S. Ishiwata, Y. Matsui, and Y. Tokura, Skyrmions with varying size and helicity in composition-spread helimagnetic alloys, *Nature Nanotechnology* **8**, 723 -728 (2013).
 - ²⁴ H. S. Park, X. Yu, S. Aizawa, T. Tanigaki, T. Akashi, Y. Takahashi, T. Matsuda, N. Kanazawa, Y. Onose, and D. Shindo, Observation of the magnetic flux and three-dimensional structure of skyrmion lattices by electron holography, *Nature Nanotechnology* **9**, 337 - 342 (2014).
 - ²⁵ A. Schlenhoff, P. Lindner, J. Friedlein, S. Krause, R. Wiesendanger, M. Weinl, M. Schreck, and M. Albrecht, Magnetic nano-skyrmion lattice observed in a Si-wafer-based multilayer system, *ACS Nano* **9**, 5908 - 5912 (2015).
 - ²⁶ O. Boulle, J. Vogel, H. Yang, S. Pizzini, D. de Souza Chaves, A. Locatelli, T. O. Montes, A. Sala, L. D. Buda-Prejbeanu, and O. Klein, Room-temperature chiral magnetic skyrmions in ultrathin magnetic nanostructures, *Nature Nanotechnology* **11**, 449 - 454 (2016).
 - ²⁷ C. Moreau-Luchaire, C. Moutafis, N. Reyren, J. Sampaio, C. Vaz, N. Van Horne, K. Bouzehouane, K. Garcia, C. Deranlot, and P. Warnicke, Additive interfacial chiral interaction in multilayers for stabilization of small individual skyrmions at room temperature, *Nature Nanotechnology* **11**, 444 - 448 (2016).
 - ²⁸ S. Woo, K. Litzius, B. Krüger, M.-Y. Im, L. Caretta, K. Richter, M. Mann, A. Krone, R. M. Reeve, and M. Weigand, Observation of room-temperature magnetic skyrmions and their current-driven dynamics in ultrathin metallic ferromagnets, *Nature Materials* **15**, 501 - 506 (2016).
 - ²⁹ G. Yu, P. Upadhyaya, X. Li, W. Li, S. K. Kim, Y. Fan, K. L. Wong, Y. Tserkovnyak, P. K. Amiri, and K. L. Wang, Room-temperature creation and spin-orbit torque manipulation of skyrmions in thin films with engineered asymmetry, *Nano Letters* **16**, 1981 - 1988 (2016).
 - ³⁰ W. Legrand, D. Maccariello, N. Reyren, K. Garcia, C. Moutafis, C. Moreau-Luchaire, S. Collin, K. Bouzehouane, V. Cros, and A. Fert, Room-temperature current-induced generation and motion of sub-100 nm skyrmions, *Nano Letters* **17**, 2703 - 2712 (2017).
 - ³¹ D. Pollard, J. A. Garlow, J. Yu, Z. Wang, Y. Zhu, and H. Yang, Observation of stable Néel skyrmions in cobalt/palladium multilayers with Lorentz transmission electron microscopy, *Nature Communications* **8**, 14761-(8) (2017).
 - ³² A. Soumyanarayanan, M. Raju, A. L. Gonzalez Oyarce, A. K. C. Tan, M.-Y. Im, A. P. Petrovic, P. Ho, K. H. Khoo, M. Tran, C. K. Gan, F. Ernult, and C. Panagopoulos, Tunable room-temperature magnetic skyrmions in Ir/Fe/Co/Pt multilayers, *Nature Materials* **16**, 898 - 904 (2017).
 - ³³ L. Cai, E. M. Chudnovsky, and D. A. Garanin, Collapse of skyrmions in two-dimensional ferromagnets and antiferromagnets, *Physical Review B* **86**, 024429-(4) (2012).
 - ³⁴ A. P. Malozemoff and J. C. Slonczewski, *Magnetic Domain Walls in Bubble Materials*, Academic Press 1979.
 - ³⁵ T. H. O'Dell, *Ferromagnetodynamics: The Dynamics of Magnetic Bubbles, Domains, and Domain Walls*, Wiley 1981.
 - ³⁶ C. Moutafis, S. Komineas, and J. A. C. Bland, Dynamics and switching processes for magnetic bubbles in nanoelements, *Physical Review B* **79**, 224429-(8) (2009).
 - ³⁷ M. Ezawa, Giant skyrmions stabilized by dipole-dipole interactions in thin ferromagnetic films, *Physical Review Letters* **105**, 197202-(4) (2010).
 - ³⁸ I. Makhfudz, B. Krüger, and O. Tchernyshyov, Inertia and chiral edge modes of a skyrmion magnetic bubble, *Physical Review Letters* **109**, 217201-(4) (2012).
 - ³⁹ S. A. Montoya, S. Couture, J. J. Chess, J. C. T. Lee, N. Kent, D. Henze, S. K. Sinha, M.-Y. Im, S. D. Kevan, P. Fischer, B. J. McMorran, V. Lomakin, S. Roy, and E. E. Fullerton, Tailoring magnetic energies to form dipole skyrmions and skyrmion lattices, *Physical Review B* **95**, 024415-(10) (2017).
 - ⁴⁰ D. A. Garanin, E. M. Chudnovsky, and X. X. Zhang, Skyrmion clusters from Bloch lines in ferromagnetic films, *Europhysics Letters* **120**, 17005-(7) (2017).
 - ⁴¹ G. Chen, A. Mascaraque, A. T. N'Diaye, and A. K. Schmid, Room temperature skyrmion ground state stabilized through interlayer exchange coupling, *Applied Physics Letters* **106**, 242404-(5) (2015).
 - ⁴² S.-Z. Lin and S. Hayami, Ginzburg-Landau theory for skyrmions in inversion-symmetric magnets with competing interactions, *Physical Review B* **93**, 064430-(16) (2016).
 - ⁴³ L. Rózsa, A. Deák, E. Simon, R. Yanes, L. Udvardi, L.

- Szunyogh, and U. Nowak, Skyrmions with attractive interactions in an ultrathin magnetic film, *Physical Review Letters* **117**, 157205-(6) (2016).
- ⁴⁴ S. von Malottki, B. Dupé, P. F. Bessarab, A. Delin, and S. Heinze, Enhanced skyrmion stability due to exchange frustration, *Nature Scientific Reports* **7**, 12229 (2017).
- ⁴⁵ J. H. Han, book: *Skyrmions in Condensed Matter*, Springer (Switzerland) 2017.
- ⁴⁶ A. Abanov and V. L. Pokrovsky, Skyrmion in a real magnetic film, *Physical Review B* **58**, R8889-R8892 (1998).
- ⁴⁷ B. A. Ivanov, A. Y. Merkulov, V. A. Stepanovich, C. E. Zaspel, Finite energy solitons in highly anisotropic two dimensional ferromagnets, *Physical Review B* **74**, 224422-(17) (2006).
- ⁴⁸ E. G. Galkina, E. V. Kirichenko, B. A. Ivanov, V. A. Stephanovich, Stable topological textures in a classical two-dimensional Heisenberg model, *Physical Review B* **79**, 134439-(8) (2009).
- ⁴⁹ E. M. Chudnovsky and D. A. Garanin, Topological order generated by a random field in a 2D exchange model, *Physical Review Letters* **121**, 017201-(4) (2018).
- ⁵⁰ E. M. Chudnovsky and D. A. Garanin, Skyrmion glass in a 2D Heisenberg ferromagnet with quenched disorder, *New Journal of Physics* **20**, 033006-(9) (2018).
- ⁵¹ I. Dzyaloshinsky, A Thermodynamic Theory of Weak Ferromagnetism of Antiferromagnetics, *Journal of Physics and Chemistry of Solids* **4**, 241-255 (1958).
- ⁵² T. Moriya, Anisotropic Superexchange Interaction and Weak Ferromagnetism, *Physical Review* **120**, 91-98 (1960).
- ⁵³ U. K. Röfller, N. Bogdanov, and C. Pfleiderer, Spontaneous skyrmion ground states in magnetic metals, *Nature* **442**, 797-801 (2006).
- ⁵⁴ S. Heinze, K. von Bergmann, M. Menzel, J. Brede, A. Kubetzka, R. Wiesendanger, G. Bihlmayer, and S. Blugel, Spontaneous atomic-scale magnetic skyrmion lattice in two dimensions, *Nature Physics* **7**, 713-718 (2011).
- ⁵⁵ A. O. Leonov and M. Mostovoy, Multiply periodic states and isolated skyrmions in an anisotropic frustrated magnet, *Nature Communications* **6**, 8275-(8) (2015).
- ⁵⁶ G. Yu, P. Upadhyaya, Q. Shao, H. Wu, G. Yin, X. Li, C. He, W. Jiang, X. Han, P. K. Amiri, and K. Wang, Room-temperature skyrmion shift device for memory application, *Nano Letters* **17**, 261-268 (2016).
- ⁵⁷ M. He, L. Peng, Z. Zhu, G. Li, J. Cai, J. Li, H. Wei, L. Gu, S. Wang, and T. Zhao, *Applied Physics Letters* **111**, 202403-(5) (2017).
- ⁵⁸ W. Jiang, P. Upadhyaya, W. Zhang, G. Yu, M. B. Jungfleisch, F. Y. Fradin, J. E. Pearson, Y. Tserkovnyak, K. L. Wang, and O. Heinonen, S. G. E. to Velthuis, and A. Hoffmann, Blowing magnetic skyrmion bubbles, *Science* **349**, 283-286 (2015).
- ⁵⁹ N. Romming, C. Hanneken, M. Memzel, J. E. Bickel, B. Wolter, K. von Bergmann, A. Kubetzka, and R. Wiesendanger, Writing and deleting single magnetic skyrmions, *Science* **341**, 636-639 (2013).
- ⁶⁰ S. Zhang, J. Zhang, Q. Zhang, C. Barton, V. Neu, Y. Zhao, Z. Hou, Y. Wen, C. Gong, O. Kazakova, W. Wang, Y. Peng, D. A. Garanin, E. M. Chudnovsky, and X. X. Zhang, Direct writing of room temperature and zero field skyrmion lattices by a scanning local magnetic field, *Applied Physics Letters* **112**, 132405-(5) (2018).
- ⁶¹ D. A. Garanin, D. Capic, S. Zhang, X. X. Zhang, and E. M. Chudnovsky, Writing skyrmions with a magnetic dipole, *Journal of Applied Physics* **124**, 113901-(8) (2018).
- ⁶² G. Berruto, I. Madan, Y. Murooka, G. M. Vanacore, E. Pomarico, J. Rajeswari, R. Lamb, P. Huang, A. J. Kruchkov, Y. Togawa, T. LaGrange, D. McGrouther, H. M. Ronnow, and F. Carbone, Laser-induced skyrmion writing and erasing in an ultrafast cryo-Lorentz transmission electron microscopy, *Physical Review Letters* **120**, 117201-(6) (2018).
- ⁶³ S. Zhang, J. Zhang, Y. Wen, E. M. Chudnovsky, and X. X. Zhang, Creation of a thermally assisted skyrmion lattice in Pt/Co/Ta multilayer films, *Applied Physics Letters* **113**, 192403-(5) (2018).
- ⁶⁴ A. Bogdanov and A. Hubert, Thermodynamically stable magnetic vortex states in magnetic crystals, *Journal of Magnetism and Magnetic Materials* **138**, 255-269 (1994).
- ⁶⁵ S. Buhbrandt and L. Fritz, Skyrmion lattice phase in three-dimensional chiral magnets from Monte Carlo simulations, *Physical Review B* **88**, 195137-(6) (2013).
- ⁶⁶ J. Hagemester, N. Romming, K. von Bergmann, E. Y. Vedmedenko, and R. Wiesendanger, Stability of single skyrmionic bits, *Nature Communications* **6**, 8455-(7) (2015).
- ⁶⁷ L. Rózsa, E. Simon, K. Palotás, L. Udvardi, and L. Szunyogh, Complex magnetic phase diagram and skyrmion lifetime in an ultrathin film from atomistic simulations, *Physical Review B* **93**, 024417-(10) (2016).
- ⁶⁸ M. Böttcher, S. Heinze, S. Egorov, J. Sinova, and B. Dupe, B-T phase diagram of Pd/Fe/Ir(111) computed with parallel tempering Monte Carlo, *New Journal of Physics* **20**, 103014-(11) (2018).
- ⁶⁹ H. Oike, A. Kikkawa, N. Kanazawa, Y. Taguchi, M. Kawasaki, Y. Tokura, and F. Kagawa, Interplay between topological and thermodynamic stability in a metastable magnetic skyrmion lattice, *Nature Physics* **12**, 62-66 (2016).